

# Advanced aspects of electromagnetic SERS enhancement factors at a hot spot

E. C. Le Ru,\* M. Meyer, E. Blackie and P. G. Etchegoin

The MacDiarmid Institute for Advanced Materials and Nanotechnology, School of Chemical and Physical Sciences, Victoria University of Wellington, Wellington, New Zealand

Received 18 September 2007; Accepted 2 December 2007

**In this paper, we discuss some advanced theoretical aspects of electromagnetic enhancement factors (EFs) in surface-enhanced Raman scattering (SERS). We focus in particular on the influence of surface selection rules (SSRs) on SERS EFs at hot spots, and the determination of SERS depolarization ratios. Both aspects could be viewed as secondary (compared to the overall magnitude of the SERS EF), but are nevertheless observable experimentally and crucial for a fundamental understanding of SERS. They also share the property that they cannot be studied within the commonly used  $|E|^4$  approximation to the SERS EFs, and appropriate tools are developed here to make predictions beyond this approximation in the case of a SERS hot spot. In addition, theoretical estimates of different types of (previously defined) EFs are provided, and their origins discussed for the typical example of a SERS substrate dominated by SERS hot spots. Finally, experimental measurements of SERS depolarization ratios are presented to support the theoretical predictions. Copyright © 2008 John Wiley & Sons, Ltd.**

**KEYWORDS:** SERS; enhancement factors; surface selection rules; depolarization ratio; hot spots

## INTRODUCTION

In a recent paper,<sup>1</sup> we have presented a comprehensive study of surface-enhanced Raman scattering (SERS) enhancement factors (EFs) wherein we dealt with several of the difficulties that produced over the years (and are still producing) wide-ranging discrepancies in EF estimations. Among them, two of the most important factors had been (1) the lack of proper normalizations of the estimations by the normal ('non-SERS') cross-sections of the probes and (2) ill-established definitions of what is actually meant by 'enhancement factor' under different experimental situations. Reference 1 provides the basic definitions of different EFs that apply to standard experimental situations, and discusses their basic properties and interconnections. It provides in addition examples of rigorous experimental measurements of these SERS EFs.

With this background in sight, we discuss here some of the more technical aspects of EFs in SERS that will add the necessary details to the general picture discussed in Ref. 1, thereby going beyond the basic aspects and the right order of magnitude. While the content of Ref. 1 is likely to appeal to a wider audience of practitioners in the field, the content of the present paper is more technical and

directed to a more specialized audience. Since the emphasis of the discussion here and in Ref. 1 is on the comparison of EFs among different substrates, we will consider only the effects of electromagnetic (EM) enhancements. Chemical enhancements in SERS can be studied at a later stage, or be avoided in practice, for example, by a careful choice of the probe. In addition, we have already shown in Ref. 1 through experimental examples that it plays a relatively minor role for some of the most widely used SERS probes.

With this motivation in mind, we review here briefly the theoretical tools required for calculating SERS EM EFs and provide a few representative examples. Particular attention is given to the influence of surface selection rules (SSRs)<sup>2,3</sup> on the SERS EFs, and associated field polarization effects. We will also focus explicitly on the case of SERS substrates containing hot spots (HSs), i.e. highly localized regions of large local field enhancement.<sup>4</sup> The properties of the substrate are then entirely dominated by the HSs. A simple model of a SERS HS will, therefore, enable us to discuss in simple terms a few otherwise complicated aspects, such as SSRs. Moreover, such HSs are common, in particular, in single-molecule SERS studies.<sup>5</sup>

Theoretical calculations of SERS EM enhancements have in the past been confined to either very simple structures (such as a sphere<sup>6</sup>) or restricted to analytical or numerical computations<sup>4,7</sup> of the local field intensity enhancement factor for modes with isotropic Raman tensors at a given

\*Correspondence to: E. C. Le Ru, The MacDiarmid Institute for Advanced Materials and Nanotechnology, School of Chemical and Physical Sciences, Victoria University of Wellington, Wellington, New Zealand. E-mail: Eric.LeRu@vuw.ac.nz

frequency  $\omega$ , namely:

$$M_{\text{Loc}}^{\text{Iso}}(\omega) = |E_{\text{Loc}}(\omega)|^2/|E_0|^2 \quad (1)$$

In the latter case, denoting excitation (laser) and Raman frequencies by  $\omega_L$  and  $\omega_R$ , respectively, the SERS EF is usually taken as:

$$F_{E4}(\omega_L, \omega_R) = M_{\text{Loc}}^{\text{Iso}}(\omega_L)M_{\text{Loc}}^{\text{Iso}}(\omega_R), \quad (2)$$

which we call the  $|E|^4$  approximation, following previous studies.<sup>8</sup> To avoid the dependence of  $F_{E4}$  on the mode energy (through  $\omega_R$ ), it is also common to neglect the Stokes shift, which then reduces to the zero-Stokes shift SERS EF in the  $|E|^4$  approximation:

$$F_{E4}^0(\omega_L) \equiv M_{\text{Loc}}^{\text{Iso}}(\omega_L)^2 = |E_{\text{Loc}}(\omega_L)|^4/|E_0|^4 \quad (3)$$

These expressions correspond to the SERS EF at a given position and are, in this sense, a special case of the single-molecule enhancement factor (SMEF), as discussed in Ref. 1. Average EFs can then be deduced by spatial averaging.<sup>4,7</sup> This approach presents many advantages:  $F_{E4}^0(\omega_L)$  is, indeed, independent of many additional parameters that could be cumbersome to take into account, such as mode energy, Raman tensor of the mode, adsorption geometry of the probe, or scattering geometry of the setup. It gives, therefore, a fairly general yardstick estimation of the SERS EFs. These advantages could also be considered as shortcomings, since they prevent us from obtaining an accurate estimate (SSRs<sup>2,3</sup> are ignored, for example) and cannot therefore be used to predict some more advanced experimental results, such as the influence of adsorption geometry or depolarization ratios.

It is possible to take into account some of these extra parameters without increasing much the complexity of the problem and it is the purpose of this paper to demonstrate this point, and link the commonly used  $|E|^4$  approximation to the rigorous definition of the SMEF given

in Ref. 1. We have recently studied the validity of the  $|E|^4$  approximation and laid the basics for calculations beyond this approximation<sup>8</sup> within the framework of classical electromagnetism. These tools provide a method to precisely determine the SERS intensity, and therefore the SMEF for a given SERS substrate, with a given incident field polarization, for a given type of Raman tensor, and a given adsorption geometry. The drawback is that the results are then highly specific to the chosen parameters and that these parameters could in principle be varied through endless combinations. Furthermore, not all these combinations might be relevant for real experimental situations. We will therefore in the following focus on a few specific examples, based on a simple model SERS HS (i.e. a very localized region of high enhancement). These examples emphasize in particular the relations between SERS EFs and SSRs.

The paper is organized as follows: First, we derive the expressions for the EM SERS EFs at a HS. We start with the SMEF in the following and briefly discuss the case of average SERS EFs. This analysis demonstrates the presence of three separate contributions to the SERS EFs, which are identified and briefly discussed. The magnitude of the SERS EF is then further discussed, before moving on to predictions beyond the  $|E|^4$  approximation. In a following section we present a detailed analysis of the surface selection rules at a SERS HS, while the next section discusses SERS depolarization ratios and provides an experimental example of the main concepts. Table 1 summarizes the main notations and acronyms used in this paper, which is presented for clarity (see also the tables in Ref. 1).

## THEORETICAL PREDICTIONS OF SERS EFS FOR A SERS HS

### Calculation of the single-molecule EF

To simplify the discussion, we focus on the specific case of a SERS hot HS. This example is relevant to many

**Table 1.** Summary of acronyms, notations, and definitions. The dependence of some of these definitions upon the following parameters is also specified: excitation wavelength ( $\lambda_L$ ), mode vibrational energy or wavenumber  $\bar{\nu}_i$ , type or symmetry of the Raman tensor  $\underline{\alpha}$ , molecular adsorption geometry  $\mathbf{e}_m$ , substrate orientation with respect to incident polarization (IP) when not averaged

Name	Acronym	Definition	Depends on
Isotropic Local Field Intensity EF	$M_{\text{Loc}}^{\text{Iso}}(\omega_L)$	$ E_{\text{Loc}}(\omega_L) ^2/ E_0 ^2$	$\lambda_L$ , IP
EF in the $ E ^4$ approximation	$F_{E4}(\omega_L, \omega_R)$	$M_{\text{Loc}}^{\text{Iso}}(\omega_L)M_{\text{Loc}}^{\text{Iso}}(\omega_R)$	$\lambda_L$ , $\bar{\nu}_i$ , IP
$F_{E4}$ at zero Stokes shift	$F_{E4}^0(\omega_L)$	$M_{\text{Loc}}^{\text{Iso}}(\omega_L)^2 =  E_{\text{Loc}}(\omega_L) ^4/ E_0 ^4$	$\lambda_L$ , IP
Maximum $M_{\text{Loc}}^{\text{Iso}}(\omega_L)$ at a hot spot	$M_{\text{Max}}^{\text{Iso}}(\omega_L)$	$M_{\text{Loc}}^{\text{Iso}}(\omega)$ for IP along HS axis ( $\theta = 0$ )	$\lambda_L$ , IP
Electromagnetic single molecule EF	EMSMEF	See Ref. 1	$\lambda_L$ , $\bar{\nu}_i$ , $\underline{\alpha}$ , $\mathbf{e}_m$ , IP
Electromagnetic SERS substrate EF	EMSSEF	See Ref. 1	$\lambda_L$ , $\bar{\nu}_i$ , $\underline{\alpha}$ , $\mathbf{e}_m$ , IP
Hot-spot axis	$\mathbf{e}_{\text{HS}}$	Unit vector along dimer axis	–
Raman polarizability tensor	$\underline{\alpha}$	See Sec. S.III of Ref. 1	–
Amplitude of $\underline{\alpha}$	$\alpha_0$	Eqn S22 of Ref. 1	–
Normalized Raman tensor	$\tilde{\alpha}$	$\underline{\alpha}/\alpha_0$	–
Surface selection rules factor	SSRF	$T(\tilde{\alpha}, \mathbf{e}_{\text{HS}}) =  \mathbf{e}_{\text{HS}} \cdot \tilde{\alpha} \cdot \mathbf{e}_{\text{HS}} ^2$	$\tilde{\alpha}$ , $\mathbf{e}_m$

experimental situations and will enable us to illustrate several important points. One should, however, bear in mind that the following expressions may not directly apply to SERS substrates where HSs are not present or do not dominate the signal (for example for single nano-particles or for some nano-lithography substrates). Although many conclusions would hold for such cases, the exact treatment might need adaptation to the specific case under consideration.

We assume that the SERS HS is formed at a small gap between two metallic objects, as illustrated schematically in Fig. 1 with the case of two (spherical) metallic particles. Following previous studies,<sup>9,10</sup> we shall further assume that the local field at the HS is always aligned along a specific direction  $\mathbf{e}_{\text{HS}}$ , independent of the incident polarization. The local field enhancement at the HS is, however, strongly dependent on the angle  $\theta$  between the incident polarization  $\mathbf{E}_0$  and the HS axis  $\mathbf{e}_{\text{HS}}$ , and the coupling to the HS is similar to that of a dipole. These general properties of SERS HSs have been studied recently elsewhere.<sup>4,9,10</sup> The local field at the HS is given by:

$$\mathbf{E}_{\text{Loc}} = \sqrt{M_{\text{Max}}}(\mathbf{e}_{\text{HS}} \cdot \mathbf{E}_0)\mathbf{e}_{\text{HS}}, \quad (4)$$

and the local field intensity enhancement factor for an isotropic mode at the HS is then<sup>9</sup>

$$M_{\text{Loc}}^{\text{Iso}}(\omega, \theta) = M_{\text{Max}}(\omega) \cos^2 \theta \quad (5)$$

These assumptions provide, to a very good approximation, a simple description of the HS formed at a gap between two spherical particles, where  $\mathbf{e}_{\text{HS}}$  is the dimer axis. Moreover, the factor  $M_{\text{Max}}(\omega)$  can also be calculated in this case using the generalized Mie theory (GMT).<sup>11</sup> These assumptions should also characterize fairly well any gap HS formed at a junction between two metallic objects, with the only

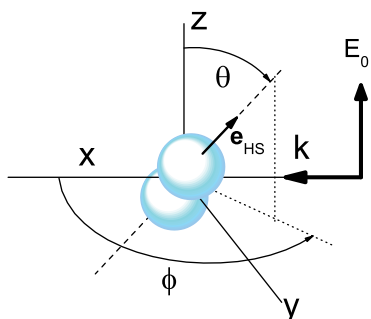


**Figure 1.** Geometrical layout for the hot spot problem. The beam is incident along the  $x$ -axis with polarization along  $z$ , and the signal is analyzed in the backscattered direction with polarization either  $\parallel$  ( $z$ ) or perpendicular ( $\perp$ ) ( $y$ ) to the incoming polarization. The main axis joining the two particles (which defines the direction of the main axis of the hot spot,  $\mathbf{e}_{\text{HS}}$ ) is defined by angles  $\theta$  (co-latitude) and  $\phi$  (longitude) in spherical coordinates. This figure is available in colour online at [www.interscience.wiley.com/journal/jrs](http://www.interscience.wiley.com/journal/jrs).

changing parameters being  $\mathbf{e}_{\text{HS}}$  and  $M_{\text{Max}}(\omega)$ . Such gap HSs have previously been studied in the literature,<sup>12,13</sup> but mostly for the case of optimal coupling ( $\theta = 0$ ).

We consider a molecule located at such a HS formed in between two nano-particles and study the SERS signal from a vibrational mode with a given Raman polarizability tensor  $\underline{\alpha}$ . The Raman polarizability is assumed to be the same for the adsorbed molecule as for the free molecule (i.e. we neglect any chemical effect). The excitation, at frequency  $\omega_L$ , is incident along the  $x$ -axis and, for simplicity, the commonly used backscattering geometry is assumed (detection along the  $x$ -axis). The incident polarization is along the  $z$ -axis and the HS axis is defined by angles  $\theta$  (co-latitude) and  $\phi$  (longitude) in spherical coordinates. The SERS signal, at frequency  $\omega_R$ , can be analyzed with a polarizer along  $\mathbf{e}_z$  (parallel,  $\parallel$ ) or  $\mathbf{e}_y$  (perpendicular,  $\perp$ ). Without polarizers, the intensity is simply the sum of the two.

For an exact treatment beyond the  $|E|^4$  approximation, we follow Ref. 8, and the ‘re-emission’ part of the SERS enhancement process is not approximated by the local field enhancement factor  $M_{\text{Loc}}^{\text{Iso}}$ , but calculated using the optical reciprocity theorem.<sup>14</sup> One can then show using Eqns (4) and (5) that the differential SERS cross-section at such a HS can be expressed as:

$$\begin{aligned} \frac{d\sigma_{\text{SERS}}}{d\Omega} &= \frac{\omega_R^4}{16\pi^2 \epsilon_0^2 c^4} |\mathbf{e}_{\text{HS}} \cdot \underline{\alpha} \cdot \mathbf{e}_{\text{HS}}|^2 \\ &\times M_{\text{Loc}}^{\text{Iso}}(\omega_L, \theta) M_{\text{Loc}}^{\text{Iso}}(\omega_R, \theta) f(\theta, \phi), \end{aligned} \quad (6)$$

where

$$f(\theta, \phi) = 1 + \tan^2 \theta \sin^2 \phi \quad (7)$$

The first term of  $f(\theta, \phi)$  corresponds to polarized detection along the  $z$ -axis (parallel), and the second along the  $y$ -axis (perpendicular). The divergence of the second term for  $\theta = \pi/2$  is irrelevant since it is then compensated by the other factors in Eqn (6) to result in a zero value.

The electromagnetic single-molecule enhancement factor (EMSMEF, defined in Ref. 1) can then be obtained, by comparison to the non-SERS cross-section, leading to:

$$\text{EMSMEF} = F_{E4}(\omega_L, \omega_R, \theta) T(\tilde{\alpha}, \mathbf{e}_{\text{HS}}) f(\theta, \phi), \quad (8)$$

where

$$T(\tilde{\alpha}, \mathbf{e}_{\text{HS}}) = |\mathbf{e}_{\text{HS}} \cdot \tilde{\alpha} \cdot \mathbf{e}_{\text{HS}}|^2, \quad (9)$$

and  $\tilde{\alpha} = \underline{\alpha}/\alpha_0$  is the normalized Raman tensor (see the definition in the Supplementary Information of Ref. 1). Through  $\tilde{\alpha}$ , we can characterize the type of Raman tensor (or Raman polarizability tensor), independently of its actual amplitude.

### Calculation of the average EF

Calculations of average SERS EFs, such as the EM SERS substrate enhancement factor (SSEF, see definition in Ref. 1),

can be quite difficult since one should, in principle, calculate the SMEF at every point on the metal surface, for every possible orientation of the probe. One simplifying assumption is to approximate the SMEF by  $F_{E4}$  (thereby ignoring orientation effects), and deduce the SSEF by averaging as in Ref. 1. As for the SMEF, this approach gives a good order-of-magnitude estimate, but misses out on both Raman tensor and field polarization effects.

To illustrate these effects, let us again consider the case of a SERS substrate containing a HS. We have recently studied the enhancement distribution around a HS<sup>4</sup> and shown that only the SERS signals from molecules at the HS contribute significantly to the total SERS intensity. It was shown as an example that ~80% of the SERS signal came from a small region covering only ~0.64% of the total substrate area, and similar conclusions were obtained experimentally.<sup>5</sup> This means that, in a first approximation, the contributing molecules are all subject to a local field oriented along the same direction, i.e. the HS axis (note that the local field intensity may still vary dramatically depending on how close a given molecule is to the HS). This assumption then enables one to treat the field enhancement and Raman tensor effects independently. The electromagnetic SERS substrate enhancement factor (EMSSEF) can then be simply derived from the single-molecule one (EMSMEF) obtained in Eqn (8) by means of:

$$\text{EMSSEF} = \{F_{E4}\}[T(\underline{\alpha}, \mathbf{e}_{\text{HS}})]f(\theta, \phi), \quad (10)$$

where {...} means spatial averaging, while [...] means averaging over the allowed orientations of the molecule (i.e. orientations compatible with the adsorption geometry) with respect to the HS axis.

As shown in Ref. 4, the spatially averaged EF in the  $|E|^4$  approximation,  $\{F_{E4}\}$ , is typically a factor 250–500 smaller than the corresponding SMEF at the HS. One can therefore expect that the EMSSEF is smaller than the EMSMEF by a similar factor. The other two terms in Eqn (10) correspond to effects beyond the  $|E|^4$  approximation, as discussed later.

Finally, note that if more than one HS is present (for large scattering volume, for example), one needs to consider possible HS-to-HS variations, and in particular changes in HS axis  $\mathbf{e}_{\text{HS}}$  and HS strength  $M_{\text{Max}}$ , and make an additional average over all those possibilities.

### The various contributions to the SERS EF

There are three distinct contributions to the EMSMEF as obtained in Eqn (8) (and similar to the EMSSEF in Eqn (10)), which illustrate many important points that apply to most SERS EFs:

- First, the most important contribution (by far) is the term  $F_{E4}(\omega_L, \omega_R, \theta) = M_{\text{Max}}(\omega_L)M_{\text{Max}}(\omega_R)\cos^4\theta$ , which corresponds to the ‘direct’ local field effect. This term essentially defines the magnitude of the EM enhancement, mostly determined by the intrinsic enhancement or

‘strength’ of the HS (the two  $M$ -factors) together with the coupling efficiency (the  $\cos^4\theta$  term). This expression shows that the  $|E|^4$  approximation is in most cases a very good estimate of the EMSMEF. It is even exact when both  $T = 1$  and  $f = 1$ . The other two terms in Eqn (8) introduce only minor changes to the magnitude of the enhancement, but do play an important role in the interpretation of SSRs and polarization effects in SERS.

- The factor  $T(\underline{\alpha}, \mathbf{e}_{\text{HS}})$  depends on the type of Raman tensor of the probe, and on its orientation with respect to the HS axis. It implies that the EMSMEF is mode dependent through the symmetry properties of a specific vibration (and possibly the adsorption geometry of the probe); this is simply a formal description of the surface selection rules<sup>2,3</sup> for a SERS HS and we call  $T(\underline{\alpha}, \mathbf{e}_{\text{HS}})$  the surface selection rules factor (SSRF). It is interesting to note that a HS presents, in a way, a much simpler scenario than SSRs on a flat surface (as studied in Refs 2, 3) because of the constancy (independent of incident field) of the polarization direction of the local field<sup>9,10</sup> (always along the HS axis). The polarization direction of the local field for a flat surface has to be obtained from Fresnel equations for the reflection process on the surface<sup>2,3</sup> (as is done in ellipsometry<sup>15</sup>) and this is a much more complicated procedure in general.
- Finally, the factor  $f(\theta, \phi)$  characterizes the polarization of the emitted (SERS) field. Note that for perfect coupling ( $\theta = 0$ ), or when the HS axis is in the plane of incidence ( $\phi = 0$ ), then  $f = 1$  and the SERS signal is fully polarized along  $z$  (incident polarization). As we shall see,  $f(\theta, \phi)$  also determines the SERS depolarization ratio that would be observed for a SERS HS or a collection of HSs.

In the rest of this paper, we discuss in more detail these contributions, and relate them to some of the other definitions of the SERS EFs introduced in Ref. 1.

### Magnitude of the EMSMEF

The previous discussion has shown that for a SERS HS, the magnitude of the EMSMEF is mostly determined by  $M_{\text{Max}}(\omega_L)M_{\text{Max}}(\omega_R)$ , with small corrections due to the SSRs and coupling efficiency of the incident polarization with the HS main axis. For an isotropic mode (and incident polarization along the HS axis), the Iso-EMSMEF (for an isotropic mode) is in fact exactly  $M_{\text{Max}}(\omega_L)M_{\text{Max}}(\omega_R)$ , i.e. the  $|E|^4$  approximation is exact. In fact, this approximation, or its simplified form  $F_{E4}^0(\omega_L)$ , has been almost exclusively used for predictions of SERS EFs in the literature (owing to its simplicity) and calculations have been carried out<sup>7,12,13</sup> for a wide range of geometries. We here give some orders of magnitude predicted by the EM theory for a SERS HS using GMT.<sup>11</sup> The isotropic local field enhancement factor for  $\theta = 0$ ,  $M_{\text{Max}}(\omega)$  is calculated for a dimer<sup>4</sup> and typically exhibits resonances (plasmon resonances) at specific wavelengths depending on the metal considered, the size of the spheres,

and their separation. The maximum value at resonance can be of the order of  $\sim 10^3 - 3 \times 10^5$  for silver, for example.<sup>4</sup> The maximum  $F_{E_4}^0$  at negligible Stokes shift is therefore in the range  $\sim 10^6 - 10^{11}$  at optimum resonance conditions, depending on the exact geometrical parameters (mostly the gap).

For non-negligible Stokes shift,  $F_{E_4}(\omega_L, \omega_R)$  exhibits a slightly blue-shifted resonance for higher energy modes, with a decreased maximum value, which depends on the width of the resonance. To illustrate this, we show in Fig. 2 the predictions of  $F_{E_4}(\omega_L, \omega_R)$  for two sets of dimer parameters (with a main dipolar interaction resonance at 550 and 655 nm, respectively) and for three different Raman shifts: 0, 600, and 1600  $\text{cm}^{-1}$ . For the resonance in the red (655 nm), which is quite broad, the maximum EF for a 1600  $\text{cm}^{-1}$  mode is reduced only by a factor of  $\sim 1.4$  compared to a mode with zero Stokes Shift. Such effects are indeed detectable experimentally, for example, in the average SERS EFs of rhodamine 6G modes.<sup>1</sup> It is also interesting to note in Fig. 2 that the magnitude of the EM enhancements remains fairly high over a wide range of wavelengths in the visible and only drops for the longest wavelengths, beyond the main dipolar interaction resonance.

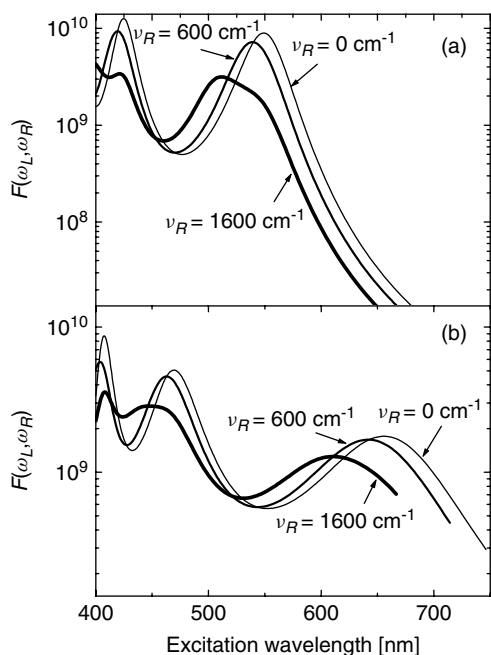


**Figure 2.** Predictions of the EM enhancement in the  $|E|^4$  approximation,  $F_{E_4}(\omega_L, \omega_R)$ , at a hot spot formed by two Ag spheres excited with polarization along the dimer axis ( $\theta = 0$ ). The results were obtained from the generalized Mie theory (GMT).<sup>11</sup> The Ag spheres, immersed in water and separated by a 2 nm gap, have radii of (a) 25 nm, and (b) 40 nm. In each case, the EFs have been computed for three different Raman shifts,  $\nu_R$ , of 0, 600, and 1600  $\text{cm}^{-1}$ .

## PREDICTIONS BEYOND THE $|E|^4$ APPROXIMATION

### Surface selection rules

We now focus on the discussion of the SSRF,  $T(\underline{\alpha}, \mathbf{e}_{\text{HS}})$ , which characterizes the SSRs at a HS in SERS conditions.

It is interesting to consider first a few representative examples of Raman tensors (we use the notation  $e_{ij} = \mathbf{e}_i \otimes \mathbf{e}_j$ , and  $\rho$  denotes the non-SERS depolarization ratio,<sup>1</sup> see also Eqn (S22) of Ref. 1 for the definition of the normalized Raman tensor  $\underline{\alpha}$ ):

- For an isotropic tensor, we have  $\underline{\alpha} = \underline{1}$  ( $\rho = 0$ ) and  $T(\underline{\alpha}, \mathbf{e}_{\text{HS}}) = 1$ , independent of the molecular orientation. This greatly simplifies the predictions, and makes the Iso-EMSMEF and the Iso-EMSSEF<sup>1</sup> the simplest tools to compare SERS substrates from a theoretical perspective, as highlighted in Ref. 1. For most other examples,  $T(\underline{\alpha}, \mathbf{e}_{\text{HS}})$  will depend on the actual orientation of the molecule with respect to the HS axis.
- For a planar isotropic tensor (i.e. a tensor isotropic along two axes and a negligible component in the third), we then have  $\underline{\alpha} = \sqrt{5/3}(e_{xx} + e_{yy})$  ( $\rho = 1/8$ ) and we can consider two extreme cases. If the molecule is adsorbed with its plane perpendicular to the HS axis, then  $T(\underline{\alpha}, \mathbf{e}_{\text{HS}}) = 0$ . The mode will be absent from the SERS spectrum. This is expected since the local field is then perpendicular to the main plane of the molecule. If the HS axis is fixed along one of the directions of the plane, then  $T(\underline{\alpha}, \mathbf{e}_{\text{HS}}) = \sqrt{5/3} \approx 1.3$ . This apparent additional enhancement (if compared to an isotropic mode) is, in a way, more related to a weaker non-SERS intensity than to a stronger SERS one. Nevertheless, such a mode will be more enhanced than an isotropic one when comparing its SERS spectrum to a non-SERS reference, i.e. its SERS EF is larger.
- For a uniaxial tensor (only one predominant component), we then have  $\underline{\alpha} = \sqrt{15/4}e_{xx}$  ( $\rho = 1/3$ ) and we consider again two extreme cases. If the axis is perpendicular to the HS axis, then  $T(\underline{\alpha}, \mathbf{e}_{\text{HS}}) = 0$ , and if it is parallel, then  $T(\underline{\alpha}, \mathbf{e}_{\text{HS}}) = \sqrt{15/4} \approx 2$ . Any intermediate values of  $T(\underline{\alpha}, \mathbf{e}_{\text{HS}})$  are in principle possible for orientations in between.

One could wonder whether it makes any sense to consider that the molecule adopts a fixed position with respect to the local field enhancement. We believe that the answer is yes, but only in some situations. The reason is that the local field at the metallic surface at a HS tends to be perpendicular to the surface. If the molecule has a preferential adsorption geometry with respect to the metal surface, then it is likely to have a preferential orientation with respect to the local field at a HS. This reasoning was also one of the main arguments for the original derivation of SSRs in SERS on planar surfaces.<sup>2,3</sup>

However, if there is no reason to believe that the adsorption geometry is fixed, then it is more physical to consider the orientation-averaged single-molecule enhancement factor

(OASMEF) (defined in Ref. 1) instead of the SMEF. Since the molecular orientation enters in Eqn (8) only through the SSRF, the OASMEF is then simply obtained by replacing  $T$  by the orientation-averaged SSRF:  $[T(\underline{\alpha}, \mathbf{e}_{\text{HS}})]$ . For a random orientation in 3D,  $[T(\underline{\alpha}, \mathbf{e}_{\text{HS}})]$  can moreover be expressed as a function of the tensor invariants as:

$$[T(\underline{\alpha}, \mathbf{e}_{\text{HS}})] = \frac{1}{1 + \rho}, \quad (11)$$

where  $\rho$  is the non-SERS standard depolarization ratio. This expression highlights one surprising (or at least counter-intuitive) result: the relative EFs (and therefore relative peak intensities) may be different in SERS conditions (as opposed to normal Raman), even when the analyte adsorbs with an entirely (in 3D) random geometry. The corrections introduced by this effect are however small (typically less than a factor of  $\sim 2$ ) since  $0 \leq \rho \leq 0.75$ . Larger corrections may be introduced by the surface selection rules for molecules adsorbing with a fixed orientation on the metal surface.

In Refs 2, 3, the SERS surface selection rules have been discussed extensively for the case of a molecule on a flat planar metallic substrate. A strong modification of the relative intensities of the Raman peak was predicted as a result of a fixed molecular orientation on the plane combined with a modified local field polarization at the metallic surface. The treatment presented above is a natural extension to the case of a SERS HS. The conclusions presented here are essentially the same, except that the local field polarization is here imposed by the HS axis, and largely independent of the excitation.<sup>9,10</sup> Moreover, the emphasis was placed here on the SERS EFs, instead of the SERS intensities, and is therefore more adapted to the comparison of SERS *vs* non-SERS peak intensities. Changes in the relative intensities of Raman peaks from non-SERS to SERS are entirely contained in the SSR factor  $T(\underline{\alpha}, \mathbf{e}_{\text{HS}})$ .

### SERS depolarization ratios

We now focus on some depolarization effects under SERS conditions that originate from the factor  $f(\theta, \phi)$ , and cannot therefore be understood within the  $|E|^4$  approximation. The first case of interest is the SERS signal from a single HS with fixed geometry. One can then study the angle dependence of the SERS signal and SERS depolarization ratio as the incident polarization is rotated. This angle dependence is described by a term  $f(\theta, \phi) \cos^4 \theta$  and the SERS depolarization ratio is  $\rho_{\text{SERS}} = \tan^2 \theta \sin^2 \phi$ . This expression is simply a consequence of the coupling of the incident polarization to the HS. It is not related in any way to the symmetry of the Raman tensor of the analyte or to its adsorption geometry.

Another example of interest is that of a colloidal solution where the orientation of the HS axis varies randomly, thereby defining the polarization averaged SERS substrate enhancement factor (PASSEF).<sup>1</sup> The two terms in the expression  $f(\theta, \phi) \cos^4 \theta$  (for parallel and perpendicular polarized detection) must then be averaged over random  $\theta$

and  $\phi$ , resulting in factors 2/5 and 2/15 (i.e. a ratio of 1/3), respectively, or their sum of 8/15 instead of  $f(\theta, \phi)$ . This can be used, for example, to express formally the polarization-averaged SSEF<sup>1</sup> in colloidal solutions (assuming all HSs are of identical strength):

$$\text{PASSEF} = \frac{8}{15} \{M_{\text{Max}}(\omega_L) M_{\text{Max}}(\omega_R)\} [T(\underline{\alpha}, \mathbf{e}_{\text{HS}})] \quad (12)$$

The magnitude of the EFs can then be approximated by the  $|E|^4$  approximation for optimum coupling ( $\theta = 0$ ), weighted by a factor 8/15 for orientation-averaging, and by the SSRF discussed previously.

One important experimental observation that also follows directly for our theoretical predictions (and that cannot be predicted within the  $|E|^4$  approximation) is that of the depolarization ratios under SERS conditions. For a collection of randomly oriented HSs, the measured depolarization ratio of all modes under SERS conditions will be 1/3, independent of the EFs or Raman tensors. This is because depolarization effects are entirely dominated by the coupling between the incident field and the HS, i.e. by  $f(\theta, \phi) \cos^4 \theta$  or its orientation-averaged equivalent. The value of 1/3 follows from the highly uniaxial nature of the HSs.

This prediction can, in fact, be observed experimentally in partially aggregated colloidal solutions, hence containing a collection of randomly oriented HSs; this is explicitly shown in Fig. 3. It is important to note that depolarization ratios in colloidal solutions must typically be studied at low colloid concentrations to avoid unwanted depolarization effects coming from multiple scattering. Figure 3 shows an explicit example for benzenethiol at a concentration of  $\sim 100 \mu\text{M}$  in partially aggregated Ag colloids (as described in Ref. 16), and diluted by a factor of  $\sim 5$  from the standard concentration produced in the Lee and Meisel method.<sup>17</sup> Measurements are carried out with an immersion ( $\times 100$ ) objective and polarization elements to obtain the parallel ( $I_{\parallel}$ ) and perpendicular ( $I_{\perp}$ ) polarized backscattered intensities at 633 nm laser excitation, respectively. Further experimental details of our system have been reported elsewhere.<sup>1,16</sup> Figs 3(a) and (b) show the Raman (non-SERS) spectra of high-concentration benzenethiol (measured inside a cell with flat windows) for  $I_{\parallel}$  and  $I_{\perp}$ , together with the depolarization ratios ( $\rho$ ) obtained from direct quotients of integrated intensities of the main peaks. The experimental values are compared to predictions of the depolarization ratios for the same modes obtained by density functional theory (DFT); calculations were performed following the same protocols as reported in Ref. 1. The overall agreement between the observed and measured depolarization ratios is excellent. On the contrary, Fig. 3(c) and (d) show the equivalent situation under SERS conditions in a diluted colloidal solution. The theoretical DFT values of the depolarization ratios are reproduced again in Fig. 3(d) for reference, together with the experimental values under SERS conditions. As can be easily appreciated from Fig. 3(d), all modes have a depolarization

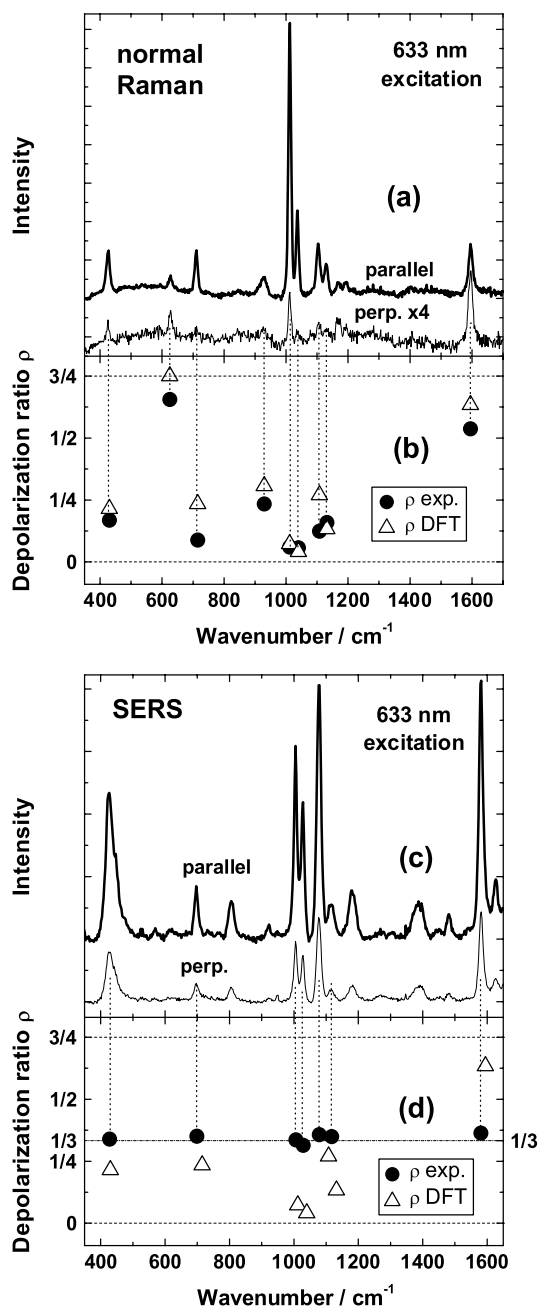


**Figure 3.** (a) Normal Raman spectra of pure benzenethiol measured in backscattering (in a cell) for parallel and perpendicular scattering configurations. In (b) we show the depolarization ratios of different modes (obtained from ratios of integrated intensities of the peaks in (a)), together with the depolarization ratios predicted for the same modes by density functional theory (DFT).<sup>1</sup> In (c) and (d) we show the corresponding situation under SERS conditions in a diluted colloidal solution. The theoretical DFT values are reproduced again in (d) for clarity. The experimental values for  $\rho$  under SERS conditions are all  $\sim 1/3$ , thus demonstrating the overriding effect of the (highly uniaxial) local field polarization at hot spots. See the text for further details.

ratio of  $\sim 1/3$  under SERS conditions. This breakdown of the normal depolarization ratio<sup>18</sup> for modes with different symmetries is then a natural consequence of the presence of HSs with highly uniaxial local fields. Despite the existence of a few reports in the literature<sup>19–22</sup> claiming that SERS at HSs can be used to probe the symmetry of modes, we show here that the polarization is predominantly determined by the highly uniaxial HS local field: a fact that has been interpreted as such in other reports,<sup>23</sup> and has already been raised in Ref. 9. The same conclusion is obtained (by adapting slightly the above argument) for a collection of HSs whose axis remain in a plane, i.e. for a dried colloidal solution on a planar substrate. Any attempt to use polarization effects in SERS (including the possibility of extending the technique to SERS optical activity<sup>9,10</sup>) cannot ignore the overriding effect of the local field.

Finally, we also note here that an important aspect of colloidal solutions is the fact that not all HSs/clusters are optimized for the resonance condition. For a fixed incident wavelength, many HSs will not be at resonance, which can reduce their SFEF by a factor of  $\sim 10$ – $100$ . This polydispersity will be apparent when measuring the analytical enhancement factor (AEF) defined in Ref. 1, which will be smaller than the SFEF or PASSEF given above, by a factor that will depend on how polydisperse and how resonant the colloidal clusters are. A reasonable value for this factor is in the range  $\sim 10$ – $100$ . Since the PASSEF is itself  $100$ – $250$  times smaller than the SMEF, the AEF can therefore be expected to be  $\sim 10^3$ – $10^4$  times smaller than the SMEF in colloidal solutions. This figure is, indeed, supported by the experimental measurements.<sup>1</sup>

## CONCLUSIONS

This paper has presented some of the additional theoretical considerations needed for a thorough understanding of SERS EFs under different experimental conditions. While being slightly more technical in nature and going one step beyond the simpler definitions in Ref. 1, these contributions prepare the ground (through estimations of the order of magnitude of the different EFs and discussion of the SSRs effects) for a direct comparison with experimental situations in real SERS applications. It also highlights some aspects of the SERS EFs that cannot be understood using the simplest  $|E|^4$  approximation, and are needed if we aim at understanding the details of the EF problem in SERS.

## REFERENCES

1. Le Ru EC, Blackie E, Meyer M, Etchegoin PG. *J. Phys. Chem. C* 2007; **111**: 13794.
2. Moskovits M. *J. Chem. Phys.* 1982; **77**: 4408.
3. Moskovits M, Suh JS. *J. Phys. Chem.* 1984; **88**: 5526.
4. Le Ru EC, Etchegoin PG, Meyer M. *J. Chem. Phys.* 2006; **125**: 204701.
5. Le Ru EC, Meyer M, Etchegoin PG. *J. Phys. Chem. B* 2006; **110**: 1944.

6. Kerker M, Wang D-S, Chew H. *Appl. Opt.* 1980; **19**: 4159.
7. Schatz GC, Young MA, Van Duyne RP. *Top. Appl. Phys.* 2006; **103**: 19 and references therein.
8. Le Ru EC, Etchegoin PG. *Chem. Phys. Lett.* 2006; **423**: 63.
9. Etchegoin PG, Galloway C, Le Ru EC. *Phys. Chem. Chem. Phys.* 2006; **8**: 2624.
10. Le Ru EC, Galloway C, Etchegoin PG. *Phys. Chem. Chem. Phys.* 2006; **8**: 3083.
11. Gérardy JM, Ausloos M. *Phys. Rev. B* 1982; **25**: 4204.
12. Xu H, Aizpurua J, Käll M, Apell P. *Phys. Rev. E* 2000; **62**: 4318.
13. Johansson P, Xu H, Käll M. *Phys. Rev. B* 2005; **72**: 035427.
14. Landau L, Lifchitz E, Pitaevskii L. *Electrodynamics of Continuous Media*. Pergamon: Oxford, 1984.
15. Azzam RMA, Bashara NM. *Ellipsometry and Polarized Light*. North Holland: Amsterdam, 1987.
16. Meyer M, Le Ru EC, Etchegoin PG. *J. Phys. Chem. B* 2006; **110**: 6040.
17. Lee PC, Meisel DJ. *J. Phys. Chem.* 1982; **86**: 3391.
18. Hayes W, Loudon R. *Scattering of Light by Crystals*. Wiley-Interscience: New York, 1978.
19. Shegai TO, Haran G. *J. Phys. Chem. B* 2006; **110**: 2459.
20. Jiang J, Bosnick K, Maillard M, Brus LE. *J. Phys. Chem. B* 2003; **107**: 9964.
21. Michaels AM, Jiang J, Brus LE. *J. Phys. Chem. B* 2000; **104**: 11965.
22. Bosnick KA, Jiang J, Brus LE. *J. Phys. Chem. B* 2002; **106**: 8096.
23. Xu H, Käll M. *Chemphyschem* 2003; **4**: 1001.